AN ANALYTICAL APPROACH TO HEAT TRANSFER FOR SLUG FLOW IN PARALLEL PLATES SUBJECTED TO CONSTANT HEAT FLUX

MUHAMMAD ABDULLAH ZAFAR GHAURI[1] *

Abstract. This document presents an analytical investigation of heat transfer characteristics in a laminar slug flow about both sides of a parallel subjected to constant heat lux. The study emphasizes on the undeveloped hydrodynamic boundary layer about the entrance region of pipe, where the velocity is approximated to be uniform. For low-Prandtl number fluids, $Pr < 1$, thermal diffusivity dominates over momentum diffusivity, thus justifying the neglect of axial conduction and viscous dissipation, The energy equation is solved using variable separation method, resulting in dimensionless temperature distribution and Nusselt's number expressions. The analysis further aims at exploring and interpreting MATLAB based results for plotting various dimensionless parameters against dimensionless axial distance and interpreting the influence of changing parameters on overall parametric distributions

Keywords. hydrodynamic boundary layer, Prandtl number, thermal diffusivity

1. Parallel Plates: Slug Flow Heat Transfer in the Entrance Region

Slug flow is defined as fluid flow in the pipe regime where small air bubble transform to large air bubbles, filling the entire pipe cross-section, with liquid slugs containing smaller entrained gas bubbles present between them. Slug flows are typically observed at low values of Prandtl number.

Considering the short unheated entrance length of tube, with small value of Prandtl number (Pr$<$ 1), where $\delta/\Delta \to 1$, implies that the momentum boundary layer can be ignored from analysis in comparison with the thermal boundary layer. The rate of development of temperature profile is faster than that of velocity profile. With this, the axial velocity can be assumed to be constant and it can be approximated as

$$v_z = V$$

where V is the average fluid velocity. The said assumption is valid only for small value of entrance length and it is not valid for large distances downstream since the velocity profile shall ultimately develop.

One may consider the two-dimensional,incompressible, steady laminar flow of a low-Prandtl number fluid flowing in the entrance region of two parallel plates as seen in 1 The fluid properties are assumed to be constant, with negligible viscous

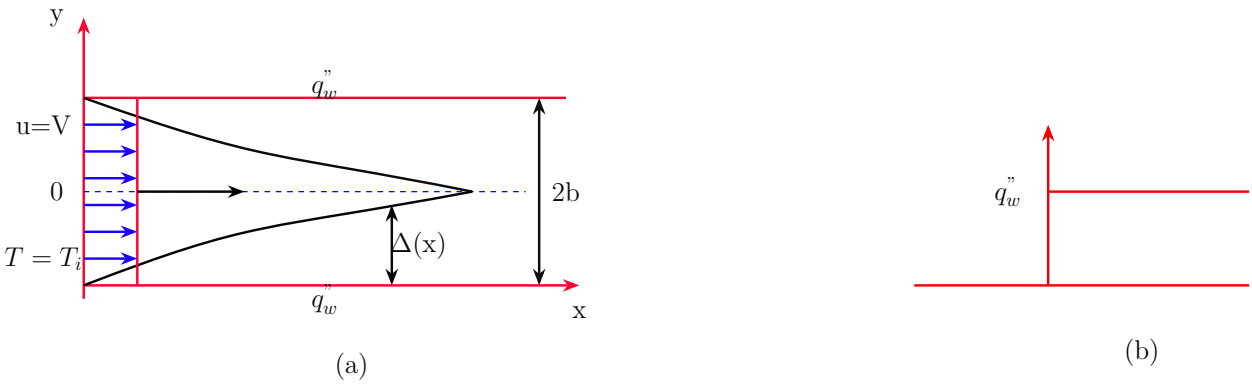


FIGURE 1. Slug flow between parallel plates (a) Thermal boundary layer development (b) Heat flux distribution

dissipation and no internal energy generation. The pipe radius is denoted as R, where the fluid enters the pipe with an initial temperature of T_i and uniform velocity V. The flow is for low-Prandtl number, where $\delta/\Delta \to 1$, the rate of development of temperature profile is faster than that of velocity profile, implying greater effect of diffusivity. With this, the axial velocity can be assumed to be constant and it can be approximated as $v_z = V$. The coordinate system is located at the duct inlet where the heating begins progressively. Heat flow gradually transforms into slug flow from the thermal pipe wall, which is maintained at uniform heat flux $q_w^{"}$. The area of duct is constant and thus, is heated about the entire length. The thermal boundary layer propagates from the entrance of duct and gradually develops along the entire length. Axial conduction and viscous dissipation are ignored from the analysis, with no energy generation. The temperature distribution and the empirical relation for the Nusselt number is to be determined.

In view of the assumptions made above, the energy equation at the entrance region is to be calculated as

$$\rho c_p V \frac{\partial T}{\partial x} = k \frac{\partial^2 T}{\partial y^2} \tag{1.1}$$

which is expressed as

$$V \frac{\partial T}{\partial x} = \alpha \frac{\partial^2 T}{\partial y^2} \tag{1.2}$$

where $\alpha = \frac{k}{\rho c_p}$ is the thermal diffusivity of plate. The corresponding boundary conditions are

$$T(0, y) = T_i \tag{1.3}$$

$$k \frac{\partial T(x, b)}{\partial y} = q_w^{"} \tag{1.4}$$

$$\frac{\partial T(x, 0)}{\partial y} = 0 \text{ (Symmetry)} \tag{1.5}$$

The heat flow is directed in negative y-direction. The dimensionless variables for broader analysis can be defined here as

$$\theta = \frac{(T - T_i)}{\left(\frac{bq_w^{"}}{k}\right)} \tag{1.6}$$

$$\eta = \frac{y}{b} \tag{1.7}$$

$$x^+ = \frac{4(x/b)}{Re_{D_H} Pr} = \frac{4(x/b)}{Pe} \tag{1.8}$$

where $Re_{D_H} = \frac{\rho D_H V}{\mu}$ is the Reynolds number, $Pr = \frac{\mu c_p}{k}$ is the Prandtl number, $D_H = 4b$ is the hydraulic diameter and $Pe = Re_{D_H} Pr$ is the Peclet number. For values of Peclet number less than 100, $Pe < 100$, axial conduction can be ignored [2]. The energy equation (Eq. 1.2) can be expressed as

$$\frac{\partial \theta}{\partial x^+} = \frac{\partial^2 \theta}{\partial \eta^2} \tag{1.9}$$

and the boundary conditions take the following shape

$$\begin{aligned}
&x^+ = 0 \qquad \theta = 0 \\
&x^+ > 0 \qquad \eta = 0 \qquad \frac{\partial \theta}{\partial \eta} = 0 \quad \text{(Symmetry)} \\
&x^+ > 0 \qquad \eta = 1 \qquad \frac{\partial \theta}{\partial \eta} = 1
\end{aligned}$$

Eq. 1.9 corresponds to a nonhomogeneous boundary condition, thus the separation of variables is not possible. The solution can be obtained from methodology discussed in [3] .

$$\theta(z^+, \eta) = \Psi(x^+, \eta) + \phi(\eta) + \varphi(x^+) \tag{1.10}$$

where $\Psi(x^+, \eta)$ is the decaying entrance region transient function, $\phi(\eta)$ is the transverse temperature variation for allowing wall heat flux to enter the fluid interface and $\varphi(x^+)$ is the axial temperature increase corresponding to the accumulated heat flux.

Substituting Eq. 1.10 into Eq. 1.9 along with corresponding boundary conditions, resulting in

$$\begin{aligned}
\frac{\partial \Psi}{\partial x^+} + \frac{d\varphi}{dx^+} &= \frac{\partial^2 \Psi}{\partial \eta^2} + \frac{d^2 \phi}{d\eta^2} \\
\theta(0, \eta) &= \Psi(0, \eta) + \phi(\eta) + \varphi(0) = 0 \\
\frac{\partial \theta(x^+, 0)}{\partial \eta} &= \frac{\partial \Psi(x^+, 0)}{\partial \eta} + \frac{d\phi(0)}{d\eta} = 0 \\
\frac{\partial \theta(x^+, 1)}{\partial \eta} &= \frac{\partial \Psi(x^+, 1)}{\partial \eta} + \frac{d\phi(1)}{d\eta} = 1
\end{aligned}$$

Splitting into individual problems

$$\frac{\partial \Psi}{\partial x^+} = \frac{\partial^2 \Psi}{\partial \eta^2} \tag{1.11}$$

$$\Psi(0,\eta) = -\phi(\eta) - \varphi(0) \tag{1.12}$$

$$\eta = 0 \qquad \frac{\partial \Psi}{\partial \eta} = 0 \tag{1.13}$$

$$\eta = 1 \qquad \frac{\partial \Psi}{\partial \eta} = 0 \tag{1.14}$$

The next set of differential equations is

$$\frac{d^2\phi}{d\eta^2} = \frac{d\varphi}{dx^+} = C \tag{1.15}$$

The functions corresponding to differential functions should be identical, therefore Eq.1.12 should correspond to a constant C since $\phi(\eta)$ and $\varphi(x^+)$ vary independently. The two differential equations, can be expressed independently as

$$\frac{d^2\phi}{d\eta^2} = C \tag{1.16}$$

The boundary conditions corresponding to Eq.1.16 are given as

$$\frac{d\phi(0)}{d\eta} = 0 \tag{1.17}$$

$$\frac{d\phi(1)}{d\eta} = 1 \tag{1.18}$$

$$\tag{1.19}$$

The nonhomogeneous boundary condition is satisfied by $\phi(\eta)$ acting on the tube wall. The second ODE is

$$\frac{d\varphi}{dx^+} = C \tag{1.20}$$

Integrating Eq. 1.16 and Eq. 1.20 such that

$$\varphi = Cx^+ + C_1$$

$$\phi = \frac{C\eta^2}{2} + C_2\eta + C_3$$

Application of boundary conditions $\phi^{'}(0) = 0$ and $\phi^{'}(1) = 1$ results in $C = 1$ and $C_2 = 0$. The remaining solutions are later expressed as

$$\varphi = x^+ + C_1$$

$$\phi = \frac{\eta^2}{2} + C_3$$

where C_1 and C_3 are unknown constants. The solution of $\Psi(x^+, \eta)$ is dependent on $\varphi(x^+)$ and $\phi(\eta)$, the constants can be arbitrarily set to 0. Hence

$$\varphi = x^+ \tag{1.21}$$

$$\phi = \frac{\eta^2}{2} \tag{1.22}$$

Solving Eq. 1.11 by assuming a product solution of form

$$\Psi = X(x^+)Y(\eta) \tag{1.23}$$

Substitution of Eq.1.23 in Eq.1.11 yields

$$\frac{d^2Y}{d\eta^2} + \lambda^2 Y = 0 \tag{1.24}$$

The corresponding boundary conditions are

$$Y^{'}(0) = 0 \tag{1.25}$$

$$Y^{'}(1) = 0 \tag{1.26}$$

$$\tag{1.27}$$

The second ODE is

$$\frac{dX}{dx^+} + \lambda^2 X = 0 \tag{1.28}$$

The solution of Eq.1.24 is

$$Y_n = A_n cos(\lambda_n \eta) + B_n sin(\lambda_n \eta)$$

evaluating the first derivative of above expression

$$Y_n^{'} = -A_n \lambda_n sin(\lambda_n \eta) + B_n \lambda_n cos(\lambda_n \eta)$$

Application of Eq.1.26 yields $B_n = 0$. Application of Eq.1.27 gives

$$A_n sin(\lambda_n)\lambda_n = 0$$

Thus

$$Y_n(\eta) = A_n \vartheta_n(\eta)$$

$$\vartheta_n(\eta) = cos(\lambda_n \eta) \quad \text{Characteristic functions}$$
$$\lambda_n = n\pi \quad \forall \qquad n = 0, 1, 2, 3 \cdots$$

The general solution of Eq.1.28 is

$$X_n(x^+) = C_n exp(-\lambda_n^2 x^+) \tag{1.29}$$

The product solution, hence takes the shape as

$$\Psi(x^+, \eta) = a_o + \sum_{n=1}^{\infty} a_n exp(-\lambda_n^2 x^+) cos(\lambda_n \eta) \tag{1.30}$$

where $a_o = A_o C_o$ and $a_n = A_n C_n$. Application of initial condition of Eq.1.11 results in

$$-\phi(\eta) - \varphi(0) = a_o + \sum_{n=1}^{\infty} a_n cos(\lambda_n \eta)$$

or

$$-\frac{\eta^2}{2} = a_o + \sum_{n=1}^{\infty} a_n cos(\lambda_n \eta)$$

$$a_o = \frac{\int_0^1 \left(-\frac{\eta^2}{2}\right) d\eta}{\int_0^1 d\eta} = -\frac{1}{6}$$

$$a_o = \frac{\int_0^1 \left(-\frac{\eta^2}{2}\right) cos(n\pi\eta) d\eta}{\int_0^1 cos^2(n\pi\eta) d\eta} = -(-1)^n \frac{2}{n^2\pi^2}$$

Equation 1.30 becomes

$$\Psi(x^+, \eta) = -\frac{1}{6} - 2\sum_{n=1}^{\infty} \frac{(-1)^n}{\lambda_n^2} exp(-\lambda_n^2 x^+) cos(\lambda_n \eta)$$

The final solution is expressed as

$$\theta(x^+, \eta) = x^+ + \frac{\eta^2}{2} - \frac{1}{6} - 2\sum_{n=1}^{\infty} \frac{(-1)^n}{\lambda_n^2} exp(-\lambda_n^2 x^+) cos(\lambda_n \eta) \tag{1.31}$$

The mean temperature of fluid T_m is

$$T_m = \frac{\int_0^b uTdy}{\int_0^b udy} = \frac{1}{b}\int_0^b Tdy$$

$$T_m = \frac{1}{b}\int_0^b \left[T_i + \frac{bq_w^{"}}{k}\theta\right] dy = T_i + \frac{bq_w^{"}}{k}\int_0^1 \theta d\eta$$

$$T_m = T_i + \frac{bq_w^{"}}{k}\int_0^1 \left[x^+ + \frac{\eta^2}{2} - \frac{1}{6} - 2\sum_{n=1}^{\infty} \frac{(-1)^n}{\lambda_n^2} exp(-\lambda_n^2 x^+) cos(\lambda_n \eta)\right]$$

$$T_m = T_i + \frac{bq_w^{"}}{k}\left[x^+ + \frac{1}{6} - \frac{1}{6} - 2\sum_{n=1}^{\infty} \frac{(-1)^n}{\lambda_n^2} exp(-\lambda_n^2 x^+) \int_0^1 cos(\lambda_n \eta) d\eta\right]$$

$$T_m = T_i + \frac{bq_w^{"}}{k}\left[x^+ + \frac{1}{6} - \frac{1}{6} - 2\sum_{n=1}^{\infty} \frac{(-1)^n}{\lambda_n^2} exp(-\lambda_n^2 x^+) \frac{sin(\lambda_n)}{\lambda_n}\right]$$

as $sin(\lambda_n) = sin(n\pi)$ is zero for all values of n and thus the mean temperature becomes

$$T_m = T_i + x^+ \frac{bq_w^{"}}{k}$$

or in dimensionless form

$$\theta_m = \frac{k(T_m - T_i)}{bq_w^{"}} = x^+ \tag{1.32}$$

The wall temperature T_w is expressed as

$$T_w = T_i + \left(\frac{bq_w^{"}}{k}\right)[\theta]_{\eta=1}$$

$$T_w = T_i + \left(\frac{bq_w^{"}}{k}\right)\left[x^+ + \frac{\eta^2}{2} - \frac{1}{6} - 2\sum_{n=1}^{\infty}\frac{(-1)^n}{\lambda_n^2}exp(-\lambda_n^2 x^+)cos(\lambda_n\eta)\right]_{\eta=1}$$

where $\cos(\lambda_n)$=$\cos(n\pi)$=$(-1)^n$. Hence, the wall temperatures become

$$T_w = T_i + \left(\frac{bq_w^{"}}{k}\right)\left[x^+ + \frac{1}{3} - 2\sum_{n=1}^{\infty}\frac{(-1)^n}{\lambda_n^2}exp(-\lambda_n^2 x^+)(-1)^n\right]$$

$$T_w = T_i + \left(\frac{bq_w^{"}}{k}\right)\left[x^+ + \frac{1}{3} - 2\sum_{n=1}^{\infty}\frac{1}{\lambda_n^2}exp(-\lambda_n^2 x^+)\right] \tag{1.33}$$

The local heat transfer coefficient is defined as

$$h = \frac{q_w^{"}}{T_w - T_m}$$

The temperature difference $T_w - T_m$ can be evaluated as

$$T_w - T_m = \left(\frac{bq_w^{"}}{k}\right)\left[\frac{1}{3} - 2\sum_{n=1}^{\infty}\frac{exp(-\lambda_n^2 x^+)}{\lambda_n^2}\right]$$

The local heat transfer coefficient takes shape as

$$h = \frac{q_w^{"}}{T_w - T_m} = \frac{q_w^{"}}{\left(\frac{bq_w^{"}}{k}\right)\left[\frac{1}{3} - 2\sum_{n=1}^{\infty}\frac{exp(-\lambda_n^2 x^+)}{\lambda_n^2}\right]}$$

$$h = \frac{q_w^{"}}{T_w - T_m} = \frac{k}{b}\frac{1}{\left[\frac{1}{3} - 2\sum_{n=1}^{\infty}\frac{exp(-\lambda_n^2 x^+)}{\lambda_n^2}\right]}$$

The local Nusselt's number can, therefore be defined for hydraulic diameter $D_H = 4b$ as

$$Nu_{D_H} = \frac{(4b)h}{k} = \frac{4}{\left[\frac{1}{3} - 2\sum_{n=1}^{\infty}\frac{exp(-\lambda_n^2 x^+)}{\lambda_n^2}\right]} \tag{1.34}$$

The axial dimensionless distance x^+ is subjected to uniform heat flux condition on both sides of plates.

The above expression of Nusselt's number is appropriate for internal flows. On plotting the Nusselt's number the asymptotic value comes as

$$Nu_{D_H} = 12$$

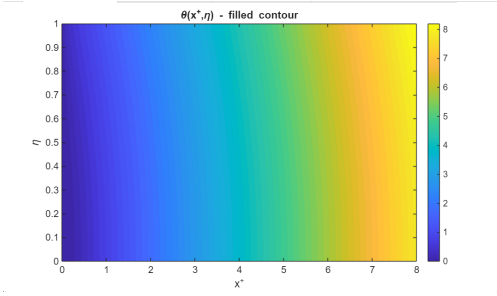


FIGURE 2. Plot of $\theta(x^+, \eta)$ as a function of dimensionless axial distance x^+

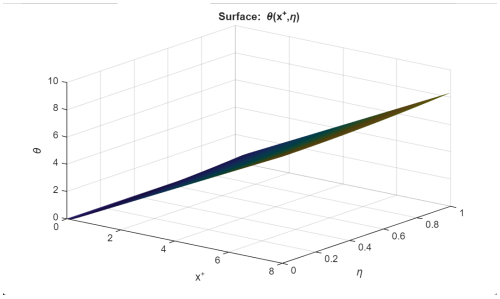


FIGURE 3. Surface plot of $\theta(x^+, \eta)$ as a function of dimensionless sxial distance x^+

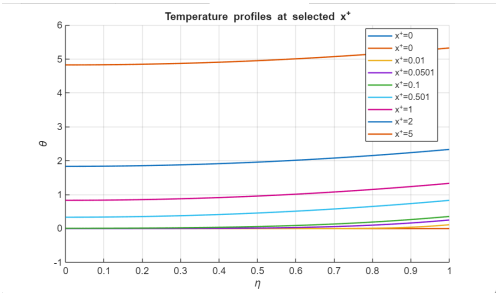


FIGURE 4. Temperature profiles at various dimensionless axial distances x^+

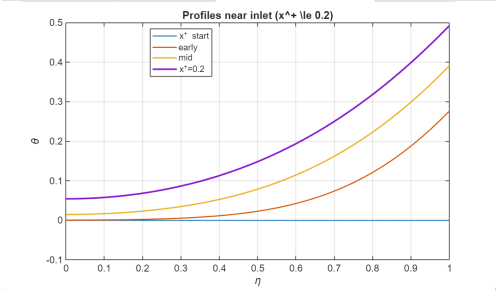


FIGURE 5. Temperature profiles close to parallel channel inlet

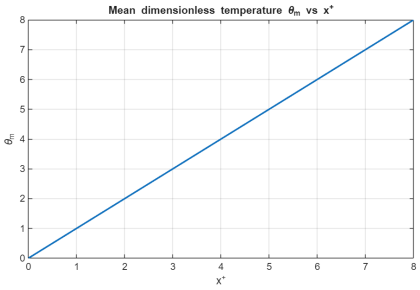


FIGURE 6. Mean dimensionless temperature as a function of dimensionless axial distance x^+

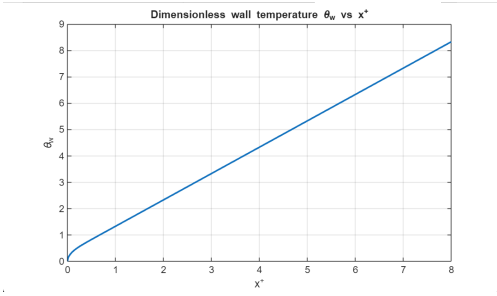


FIGURE 7. Dimensionless wall temperature as a function of dimensionless axial distance x^+

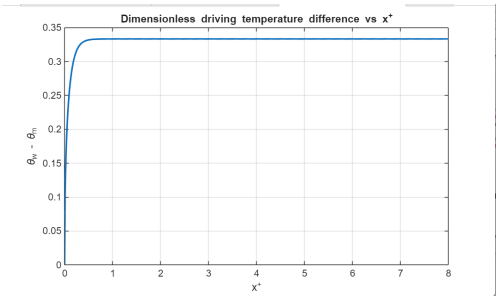


FIGURE 8. Dimensionless driving temperature difference $(T_w - T_m)$ as a function of dimensionless axial distance x^+

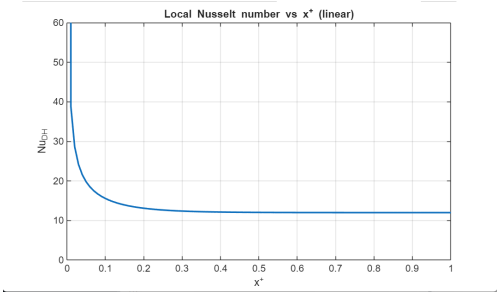


FIGURE 9. Local Nusselt's number as a function of dimensionless axial distance x^+

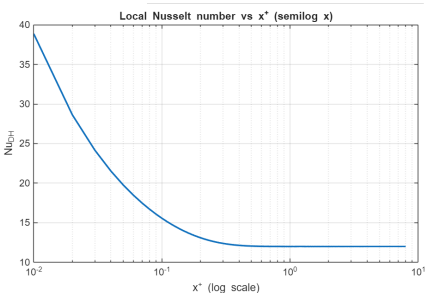


FIGURE 10. Local Nusselt's number as a function of semi-logarithmic dimensionless axial distance x^+

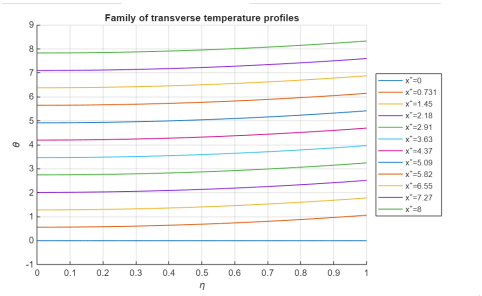


FIGURE 11. Various transverse temperature profiles

CONCLUSION

The analytical solution derived for laminar slug flow between parallel plates under a uniform wall heat flux provides a compact, physically transparent description of thermal development in the entrance region. Separation into a steady axial term, a transverse polynomial, and a rapidly decaying transient enables exact representation of the dimensionless temperature field as $\theta(x^+, \eta) = x^+ + \frac{\eta^2}{2} - \frac{1}{6} - 2\sum_{n=1}^{\infty} \frac{(-1)^n}{\lambda_n^2} exp(-\lambda_n^2 x^+) cos(\lambda_n \eta)$ from which closed-form expressions for the mean temperature and wall temperature follow. The mean dimensionless temperature grows linearly with axial distance $\theta_m = x^+$ while the wall–mean temperature difference controls the local heat-transfer coefficient leading to the

compact Nusselt relation $Nu_{D_H} = \frac{(4b)h}{k} = \frac{4}{\left[\frac{1}{3} - 2\sum_{n=1}^{\infty} \frac{exp(-\lambda_n^2 x^+)}{\lambda_n^2}\right]}$ This expression captures the strong entrance effect: very high local heat transfer near x^+ approaching 0, and relaxing toward the well-defined asymptote $Nu_{D_H} = 12$ as the transient terms vanish. The analytical solution is particularly valuable for low-Prandtl fluids where axial conduction is negligible and provides reliable benchmark data for validating numerical simulations and guiding compact models for thermal management.

References

1. , Onur N. (2023). Index. In Introduction to Convective Heat Transfer, N. Onur (Ed.). https://doi.org/10.1002/9781119766797.index
2. , Kays, W.M., Crawford, M.E., and Weigand, B. (2005). Convective Heat and Mass Transfer. McGraw-Hill.
3. , Burmeister, L.C. (1993). Convective Heat Transfer, 2e. Wiley. https://www.wiley.com/en-be/Convective+Heat+Transfer%2C+2nd+Edition-p-9780471577096

[1] School of Mechanical and Manufacturing Engineering (SMME), National University of Sciences and Technology (NUST), Islamabad Capital Territory, 44000, Pakistan

Email address: mghauri.ug22smme@student.nust.edu.pk